

Design and management of lithium-ion batteries: A perspective from modeling, simulation, and optimization

Qian-Kun Wang(王乾坤), Jia-Ni Shen(沈佳妮), Yi-Jun He(贺益君), Zi-Feng Ma(马紫峰)

Citation: Chin. Phys. B . 2020, 29(6): 068201 . **doi:** 10.1088/1674-1056/ab90f8
Journal homepage: http://cpb.iphy.ac.cn; http://iopscience.iop.org/cpb

What follows is a list of articles you may be interested in

Influence of fluoroethylene carbonate on the solid electrolyte interphase of silicon anode for Li-ion batteries: A scanning force spectroscopy study

Jieyun Zheng(郑杰允), Jialiang Liu(刘家亮), Suijun Wang(王绥军), Fei Luo(罗飞), Liubin Ben(贲留斌), Hong Li(李泓)
Chin. Phys. B . 2020, 29(4): 048203 . **doi:** 10.1088/1674-1056/ab7b54

Improved electrochemical performance of $Li(Ni_{0.6}Co_{0.2}Mn_{0.2})O_2$ at high charging cut-off voltage with $Li_{1.4}Al_{0.4}Ti_{1.6}(PO_4)_3$ surface coating

Yi Wang(王怡), Bo-Nan Liu(刘柏男), Ge Zhou(周格), Kai-Hui Nie(聂凯会), Jie-Nan Zhang(张杰男), Xi-Qian Yu(禹习谦), Hong Li(李泓)
Chin. Phys. B . 2019, 28(6): 068202 . **doi:** 10.1088/1674-1056/28/6/068202

Improved electrochemical performances of high voltage $LiCoO_2$ with tungsten doping

Jie-Nan Zhang(张杰男), Qing-Hao Li(李庆浩), Quan Li(李泉), Xi-Qian Yu(禹习谦), Hong Li(李泓)
Chin. Phys. B . 2018, 27(8): 088202 . **doi:** 10.1088/1674-1056/27/8/088202

Multi-scale computation methods: Their applications in lithium-ion battery research and development

Siqi Shi(施思齐), Jian Gao(高健), Yue Liu(刘悦), Yan Zhao(赵彦), Qu Wu(武曲), Wangwei Ju(琚王伟), Chuying Ouyang(欧阳楚英), Ruijuan Xiao(肖睿娟)
Chin. Phys. B . 2016, 25(1): 018212 . **doi:** 10.1088/1674-1056/25/1/018212

Lithium-ion transport in inorganic solid state electrolyte

Jian Gao(高健), Yu-Sheng Zhao(赵予生), Si-Qi Shi(施思齐), Hong Li(李泓)
Chin. Phys. B . 2016, 25(1): 018211 . **doi:** 10.1088/1674-1056/25/1/018211

TOPICAL REVIEW — Advanced calculation & characterization of energy storage materials & devices at multiple scale

Design and management of lithium-ion batteries: A perspective from modeling, simulation, and optimization*

Qian-Kun Wang(王乾坤), Jia-Ni Shen(沈佳妮), Yi-Jun He(贺益君)†, and Zi-Feng Ma(马紫峰)

Department of Chemical Engineering, Shanghai Jiao Tong University, Shanghai 200240, *China*

(Received 1 November 2019; revised manuscript received 13 April 2020; accepted manuscript online 7 May 2020)

Although the lithium-ion batteries (LIBs) have been increasingly applied in consumer electronics, electric vehicles, and smart grid, they still face great challenges from the continuously improving requirements of energy density, power density, service life, and safety. To solve these issues, various studies have been conducted surrounding the battery design and management methods in recent decades. In the hope of providing some inspirations to the research in this field, the state of the art of design and management methods for LIBs are reviewed here from the perspective of process systems engineering. First, different types of battery models are summarized extensively, including electrical model and multi-physics coupled model, and the parameter identification methods are introduced correspondingly. Next, the model based battery design methods are reviewed briefly on three different scales, namely, electrode scale, cell scale, and pack scale. Then, the battery model based battery management methods, especially the state estimation methods with different model types are thoroughly compared. The key science and technology challenges for the development of battery systems engineering are clarified finally.

Keywords: lithium-ion batteries, modeling, design, management

PACS: 82.47.Aa, 82.47.Wx **DOI:** 10.1088/1674-1056/ab90f8

1. Introduction

Nowadays, the lithium-ion batteries (LIBs) have been the most favored secondary batteries in both mobile and stationary applications.[1,2] Compared to other kinds of secondary batteries, LIBs have the advantages of high gravimetric and volumetric energy and power density, low self-discharge rate, and long cycle and calendar lifetime.[3] When used in practice, the battery performance requirements are usually different under different application scenarios. In the electric vehicles application, the batteries are required to provide the longer driving range and higher charging rate. In the energy storage system application, the batteries are preferred with longer service life and operational stability.[4] Whatever, the pursuit of high specific energy, long service life, and high security batteries is and will still be the hot scientific issue in this field.[5] To achieve this goal, on one hand, the new materials and the new chemistry systems are developed constantly; on the other hand, more and more attention is paid to the advanced battery design methods, battery manufacturing techniques, and battery management strategies, which have shown great effects on the overall battery performance.

The process systems engineering (PSE) is an interdisciplinary research field, which focuses on the development and application of modeling, simulation, and optimization methods to assist in the optimal design, operation, control, scheduling, and planning of complex processes.[6] Inspired by its application in petrochemical industry and pharmaceutical industry, some studies proposed the PSE concept to the battery industry with the intent of accelerating the design optimization process and realizing optimal operation of LIBs.[7,8]

This works aims to present a systematical review of the battery modeling, simulation, and optimization methods in existing literatures, especially focusing on their applications in battery design and management. The remainder of this article is structured as follows. First, different battery modeling and simulation approaches for both electrical model and multi-physics coupled model are summarized, and the parameter identification methods are introduced correspondingly. Then, the model based battery design methods on three different scales are introduced extensively, namely, electrode scale, cell scale, and pack scale. Furthermore, the battery model based battery management methods, especially the state estimation methods combined with different model types are thoroughly compared. Finally, the key science and technology challenges for the development of battery system engineering are clarified, in the hope of providing some inspirations to the research in this field.

2. Modeling and simulation of LIBs

The importance of battery modeling lies in the fact that it can describe the internal and external battery characteris-

*Project supported by the National Key R&D Program of China (Grant No. 2018YFB0905000) and the National Natural Science Foundation of China (Grant No. 21978166).

†Corresponding author. E-mail: heyijun@sjtu.edu.cn

© 2020 Chinese Physical Society and IOP Publishing Ltd

tics varying with different structures and different operation conditions, which is great helpful to perform the optimal design and management of LIBs. Since the battery is a system for the transformation and storage of electric energy, the essential function of a battery model is to describe the relationship between the current and voltage response. The existing battery electrical models can be broadly divided into three categories: equivalent circuit model (ECM), electrochemical model, and empirical model.[8,9] The ECM, composed of electrical elements such as resistance and capacitance, has been widely used in battery management system (BMS),[10] as it provides trade-off between model complexity and accuracy. The electrochemical model, which describes the battery behaviors based on the differential algebraic equations,[11] is much more complex. And thus, it is mainly used in the battery design applications. The empirical model is simple and calculation efficient, however, the accuracy is usually too low to the unseen battery operating regions.[12]

Besides the battery electrical response modeling, the battery thermal behaviors are also concerned by researchers.[13] Temperature is one critical factor on battery performance. On one hand, the low temperature could restrict the diffusion and reaction rate, which would result in the larger internal resistance and the lower power capability. On the other hand, the excessive temperature could accelerate the side reaction rate, which would accelerate battery degradation and even cause thermal runaway.[14,15] Therefore, it is necessary to develop the accurate electrical–thermal coupled models for assisting in the optimal design and management of LIBs, especially for the large format battery.[16] However, the accurate description and prediction of battery thermal behaviors are usually difficult. The main reason is that the heat generation mechanism of batteries is complex and the nondestructive measurement of the battery temperature distribution is still a challenging task.

Furthermore, the parameters in electrical model or electrical-thermal coupled model would continuously vary with the battery degradation, which would result in poor prediction performance of the electrical and thermal behaviors.[17] Therefore, it is necessary to account for the battery degradation in the view of the whole battery service life. It means that the thermal and mechanical stress induced battery degradation model could be developed and coupled with the electrical–thermal model, or aging related electrical and thermal parameters should be properly online adjusted with the battery degradation.

2.1. Electrical model

2.1.1. Equivalent circuit model

The ECMs can be established based either on the battery charge/discharge curves or on the electrochemical impedance spectroscopy (EIS). The former is named as time-domain ECM, while the latter is called as frequency-domain ECM. Both types of ECMs have been widely studied in the literatures.[18–20] Figure 1 shows four typical kinds of ECMs for LIBs.

The Rint model is the simplest ECM, composed of one resistor and one voltage source connected in series, as shown in Fig. 1(a). The voltage response of this model can be described as follows:

$$U_{\mathrm{T}} = U_{\mathrm{OC}} - IR, \tag{1}$$

where U_{T} is the terminal voltage of the battery; U_{OC} is the open circuit voltage (OCV); I is the current through the battery; and R is the internal resistance. As the Rint model is simple, it has low terminal voltage simulation accuracy, especially when the current changes quickly and the relaxation phenomenon appears. The relaxation phenomenon could arise from the interface capacitance between electrolyte and solid material, as well as the solid and liquid phase diffusion properties.[18] To improve the simulation accuracy under relaxation condition, the ECMs with parallel resistors and capacitors network are proposed.

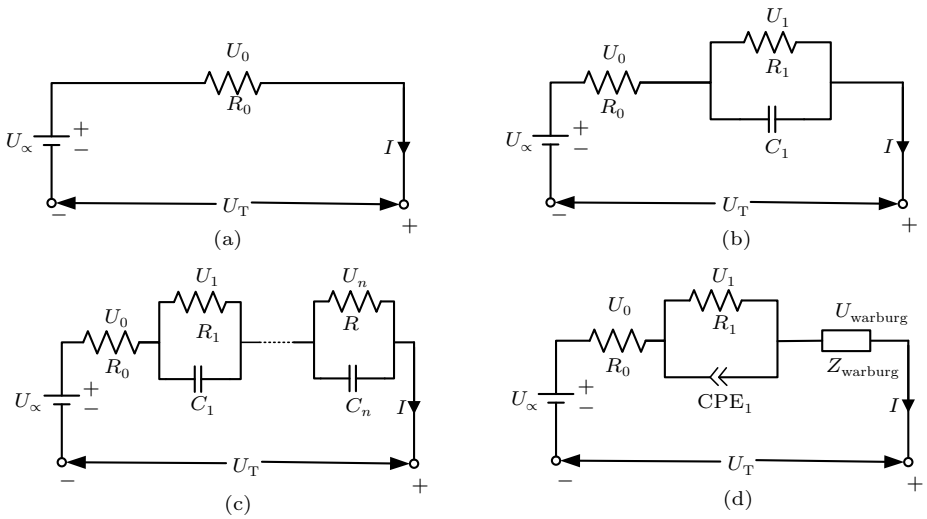


Fig. 1. Four typical kinds of ECMs for LIBs: (a) Rint model; (b) Thevenin model; (c) *n*-*RC* model; (d) frequency domain ECM.

Figure 1(b) shows the Thevenin model, composed of Rint model and one-*RC* network. The general framework of time-domain ECM with *n*-*RC* circuit is shown in Fig. 1(c). The terminal voltage of an *N*-order Thevenin model can be calculated by the following equations:

$$U_0 = IR_0, \tag{2}$$

$$\frac{\mathrm{d}U_i}{\mathrm{d}t} = -\frac{U_i}{R_iC_i} + \frac{I}{C_i}, \tag{3}$$

$$U_\mathrm{T} = U_\mathrm{OC} - U_0 - \sum_{i=1}^{N} U_i, \tag{4}$$

where U_0 is the voltage drop across R_0, and U_i is the voltage drop of the i-th *RC* pair. In theory, the increasing order of the *RC* networks can bring the better model fitting performance, but the computational cost would increase and the over-fitting risk may rise as well.

Figure 1(d) shows the general architecture of frequency-domain ECMs. The frequency-domain ECM can be established with the EIS or with time-domain test like dynamic stress test and hybrid pulse power characterization test.[19] Usually, the frequency-domain ECMs contain the constant phase element (CPE) and the Warburg element, where a parallel pair of resistor and CPE is also called ZARC element. In some cases, especially in the application of half-cell, the EIS is an effective tool to separate physic-chemical processes in different time constants, such as the solid diffusion process, the electrochemical reaction process, and the solid electrolyte interface (SEI) film dynamics.[20] However, in the application of full-cell, the separation of different dynamic steps is more difficult, and the meaning of the circuit parameters could be more ambiguous. Even though, the parameters of the frequency-domain ECM are significant indicators for battery aging state.

Unlike the time-domain ECMs, some elements in the frequency-domain ECMs are defined in the frequency domain, such as the ZARC element and Warburg element. By applying to the time-domain charge/discharge operation, one way is to convert the ZARC and Warburg elements into series *RC* pairs, where the number of *RC* pairs is selected based on the balance between calculation complexity and approximation accuracy.[21,22] Another way is to use the fractional order calculus method, which transfers the frequency-domain ECM to a fractional order model.[23,24] In some studies, the hysteresis phenomenon is considered, and a hysteresis model is added. The hysteresis phenomenon may originate from the existence of several possible thermodynamic equilibrium potentials or arise from the lithium ion uneven distribution limited by diffusion, as a result, the relationship between OCV and state of charge (SOC) is path dependent.[25,26] As numerous ECMs have been proposed, researchers have tried to do comparative studies on the performances of different kinds of ECMs, not only for dynamic simulation applications[26] but also for the management applications.[27]

It is worth noted that the analytical solution could be easily obtained for the ordinary differential equations (ODEs) based time-domain ECMs. Hence, the numerical calculation of ECMs can be simply and efficiently performed, which would be helpful to carry out online ECM based state estimation and operation control in BMS.

2.1.2. Electrochemical model

The pseudo-two-dimensional (P2D) model proposed by Newman *et al.*[11] is the most famous electrochemical model for LIBs, which is also referred as Doyle–Fuller–Newman model.[28] The P2D model adopts the partial different equations (PDEs) to describe the mass conservation and charge conservation in the solid and liquid phases, and uses the Butler–Volmer (B–V) equation to describe the electrochemical reaction at the active material/electrolyte interface. These equations can be easily obtained from related references[11,28] and will not be listed here.

The original P2D model neglects the current distribution at the current collectors, as they have relative high electrical conductivity comparing to the active materials and electrolyte. This assumption helps to build a simple model, while is unable to describe the non-uniform performance at the electrode plane region. To extend the P2D model to a higher dimension, two different approaches have been proposed. One is to use a number of P2D sub-models that are connected in parallel by the current collector. It is assumed that no mass transfer between each sub-model, and the terminal voltage and current through each sub-model are governed by the charge balance equations of the current collector.[29] The other is to extend the original governing equations to the 3D form in which the ions and electronics can transfer not only in the electrode thickness direction but also in the in-plane direction.[30] Although the extended P2D models have higher computational complexity, they provide a possibility to investigate the non-uniform distributions of current density and active material usage in the electrode plane direction. With such models, one can study the effects of cell design factors such as the tab location, tab size, and the cell size.

As solving the problem of nonlinear PDEs is time consuming, various simplification methods of P2D model have been proposed.[31] The single particle (SP) model is the most popular one among them. It is assumed that the solid phase conductance is high enough and the lithium ion concentration distribution in the electrolyte phase can be neglected. As a result, the particles on the same electrode have the same properties, and then each electrode can be treated as a single particle. In the SP model, the particle surface current density is obtained directly based on the applied current and the surface area of each electrode. The electrochemical reaction at each electrode is modeled by the B–V equation. The voltage drop

through the electrolyte, solid state matrix, and current collector is simulated using a lumped resistor.[32,33] Since the assumption of uniform electrolyte concentration might produce a low simulation accuracy, especially under large C-rate conditions, some researchers take the electrolyte concentration into consideration, and then re-add the governing equations with the mass and charge conservation equations in the liquid phase.[34,35]

For effectively solving the P2D model, different numerical methods have been proposed. The finite-difference method (FDM) is the first adopted one, which has been implemented in Dualfoil.[36] The finite-volume method (FVM) and finite-element method (FEM) are used successively. Although the implementation of these methods requires the strong mathematical foundation and programming ability, benefiting from the development of commercial computing software, the simulation based on P2D model is much easier for today's researchers. For the SP model, besides the aforementioned numerical methods, the analytical solution can be obtained under some specific operation conditions by applying a polynomial approximation for the solid concentration in the solid state diffusion equations.[37] Generally, the increase of both discrete node number and model dimension would lead to higher computational complexity, and the detailed discussion can be referred to the study of Ramadesigan *et al.*[38]

2.1.3. Empirical model

The empirical models only focus on the external current–voltage response rather than the internal electrical or electrochemical mechanism. Shepherd model, Unnewehr universal model, and Nernst model are three typical empirical models.[12] Although the empirical models have concise mathematical forms and high calculation efficiency, they usually have poor generalization performance.

Nowadays, with the great development in the area of machine learning and artificial intelligence, more advanced data-driven empirical models, e.g., support vector machine[39] and neural network,[40] have been proposed to perform modeling of LIBs. These data-driven models could usually provide better prediction accuracy than the traditional empirical models. However, these black-box models are hard to be understood and the model complexity is relatively high. Moreover, to obtain a robust data-driven model, massive high-quality training data are needed, which are high cost in practice. Until now, the studies on data-driven models lack a comprehensive comparison on model accuracy and calculation complexity. However, compared to the ECM and electrochemical model, the simulation of the empirical model, described as analytical forms, is usually much easier and more efficient.

2.2. Multi-physics coupled model

The heat generation inside battery usually has great impact on the battery temperature, which could consequently seriously influence the whole battery operation performance.[41] To accurately model the heat generation process, Bernardi *et al.*[42] proposed a general equation, which can calculate the heat generation rate from different heat sources, including electrochemical reactions, phase changes, mixing effects, and Joule heating. Although the general equation has high accuracy, it is usually difficult and time-consuming to accurately obtain all heat generation sources. Hence, a simplified version of Bernardi's equation has been developed. By neglecting the heat generations from phase changes and mixing effects, and regarding the heat capacity as a constant, the heat sources in the simplified Bernardi's equation could be summarized into two parts, i.e., reversible and irreversible heat. The irreversible heat is mainly caused by over potential during operation including ohmic losses, charge-transfer over potentials, and mass transfer limitations. The reversible heat, also called as entropic heat, is related to the entropy change of the active material at both positive and negative electrodes.

Battery degradation occurs not only during the operation[43,44] but also during the storage,[45] which are referred as cycle aging and calendar aging, respectively.[46,47] A battery consists of several components, i.e., current collectors, positive electrode, negative electrode, separator, and electrolyte. Due to the internal and external factors, each component has the risk of failure during the battery service life. However, no matter what the specific failure mechanism, they all induce two phenomena, i.e., capacity fading and resistance increasing.[17,48–50] At the negative electrode, the formation, growth, and updating of the SEI could consume the cycleable lithium and electrolyte, which would cause the reduction of capacity and liquid phase volume fraction as well as the increase of the transportation resistance in electrolyte. Moreover, lithium plating occurring at negative electrode would contribute to the capacity fading, especially at the end of battery life.[51] In addition, the crack evolution caused by the mechanical stress during lithium insertion/extraction could result in capacity loss.[52–55] At the positive electrode, the main degradation mechanisms include the solvent oxidation and the active material loss. The solvent oxidation occurs as a result of high voltage operation, which may cause film formation at the interphase of positive electrode/electrolyte. The low electrical conductivity of the formatted interface film may lead to the loss of electronic contact between primary particles and result in resistance increase.[56] The active material loss is caused by the material dissolution, structural degradation, and fracture propagation throughout the lithium insertion/extraction.[57,58]

To simulate the multi-physics response of batteries, different types of multi-physics coupled models have been devel-

oped. Figure 2 shows the coupling strategies among different models. The electrical model usually simulates the current–voltage response behavior, and calculates the heat generation rate and electrical dependent side reaction rate for providing the inputs of thermal model and aging model, respectively. The thermal model obtains the heat generation rate from both electrical model and aging model, and provides the temperature dependent electrical and aging parameters to the electrical model and aging model, respectively. The aging model simulates the aging behavior and provides the aging dependent electrical parameters and heat generation rate for the electrical model and the thermal model, respectively.

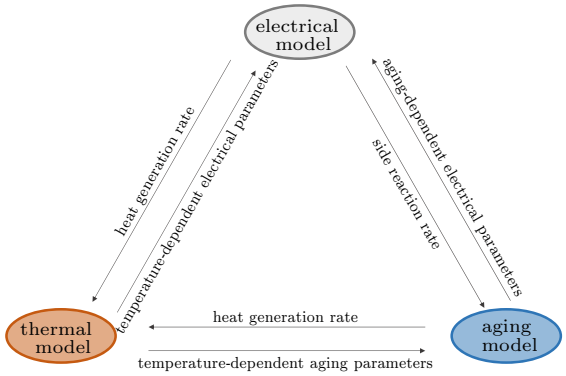


Fig. 2. Coupling strategies among battery multi-physics models.

2.2.1. Electrical–thermal coupled model

Many kinds of pure thermal models have been developed for LIBs, such as 2D thermal model[59] and 3D thermal model.[60] In a pure thermal model, the heat generation term is usually determined empirically, which would result in poor prediction performance for unseen modeling region. Therefore, the electrical–thermal coupled model needs to be developed, in which the heat generation rate could be predicted accurately based on the electrical model. There are mainly two kinds of electrical-thermal coupled models: ECM–thermal coupled model and electrochemical–thermal coupled model. In both of them, the ECM and electrochemical models can be extended to multi-dimensions, and the thermal model also can be established as 0D, 1D, 2D, and 3D. Generally, with the higher dimension, the model accuracy would improve, but the computational cost would correspondingly increase. Hence, to meet specific application requirement, the coupled models with suitable coupling strategies could be developed.

Among the ECM–thermal coupled models, the lumped parameters ECM–0D thermal model is most widely studied due to its high calculation efficiency.[61] The lumped parameter ECM–1D thermal model and lumped parameter ECM–3D thermal models have been developed for detailed thermal characteristics description of pouch type cells.[62] The higher-dimension ECM is used to better model the electrical properties. For example, 2D ECM–2D thermal model[63–65] and 2D ECM–3D thermal model[66–69] were proposed for the simulation of pouch type battery, in which the potential and current density distribution on the electrodes can be obtained using the 2D ECM.

Among the P2D electrochemical–thermal coupled models, the P2D electrochemical–0D thermal coupled model has been constructed for the battery state estimation. However, as the numerical solution of complex electrochemical model is time consuming, its online application relies on the development of efficient solving algorithms and the model reduction methods such as orthogonal decomposition and orthogonal collocation.[70–72] The P2D electrochemical–thermal coupled models with higher dimension are usually used for battery design purpose. Thermal models with higher dimension are developed to simulate the temperature distribution, like P2D electrochemical–1D thermal coupled model[73,74] and P2D electrochemical–3D thermal coupled model.[75–78] Electrochemical models with higher dimension are also developed to study the non-uniform property in the electrode plane, such as 2D electrochemical–thermal coupled model[79] and 3D electrochemical–thermal coupled model.[80–83] In these studies, the P2D models are either directly extended to higher dimension,[80,81] or implemented with parallel strategy.[82,83]

The SP electrochemical–0D thermal coupled model is the most widely studied SP–thermal coupled model,[84,85] which favors the online application.[86] Also, there are some studies about the SP–thermal coupled model with higher dimension. Baba *et al.*[87] proposed an SP electrochemical–3D thermal coupled model to simulate the electrical and thermal distribution of a cylindrical cell, in which the SP model was connected in parallel between the current collector pair. The similar model was also adopted by Darcovich *et al.*[88] in the modeling of prismatic cells.

2.2.2. Electrical–degradation coupled model

To accurately model the long-term battery behaviors, the degradation effect during the battery service life needs to be properly included. Some studies regard the side reactions as the dominant origin of degradation and then couple this process with different battery models. Safari *et al.*[89] proposed an SP electrochemical–degradation coupled model, in which the growth of SEI was considered as the main capacity fading source and the solvent diffusion in the SEI film and solvent-reduction kinetics were modeled to determine the side reaction rate. Lin *et al.*[90] proposed a P2D electrochemical–degradation coupled model for a graphite/$LiMn_2O_4$ cell, in which side reactions containing Mn dissolution in cathode, SEI growth and Mn deposition in anode, electrolyte oxidation and salt decomposition in liquid phase were model quantitatively. Pinson *et al.*[91] proposed an SP electrochemical–degradation coupled model, in which only the SEI related aging mechanism was considered. When apply to the porous

electrodes, the simulation results showed that the growth of SEI varies slightly throughout the electrode, even at high rates. Delacourt *et al.*[92] also proposed an SP electrochemical–degradation coupled model for graphite/$LiFePO_4$ cell, in which the side reaction kinetics and solvent diffusion limitations at both electrodes were taken into account. A pseudo 3D electrochemical–degradation coupled model was proposed by Awarke *et al.*,[93] in which the degradation phenomenon was modeled by the SEI growth occurring in the anode. The non-homogeneous SEI growth arising from non-uniform current distribution was analyzed, while the temperature effects were not considered.

The stress evolution during lithium intercalation/deintercalation is regarded as another important origin of battery degradation. Although some studies have coupled the diffusion-induced stress model with a P2D[94,95] or SP model,[96] the degradation phenomenon is not explicitly associated with stress. In addition, some efforts have been taken to simulate the effects of stress on SEI fracture[97] and particle crack[98,99] on particle scale, which makes it possible to develop a universal degradation model for different types of batteries. To take both side reactions and stress effects into consideration, some efforts have been taken to combine the SP model with stress and side reactions to give a comprehensive simulation on battery degradation.[100–102]

2.2.3. Electrical–thermal–degradation model

To better describe the electrical and thermal dynamics behaviors during the whole LIBs service life, the electrical–thermal–degradation models have been developed in recent years. Xie *et al.*[103] proposed a P2D electrochemical–1D thermal–degradation coupled model to describe the dynamics behaviors of graphite/$LiMn_2O_4$ cell, in which the SEI film related side reactions in the negative electrode were considered. Lamorgese *et al.*[104] adopted the similar model for the graphite/$LiCoO_2$ cell. Yang *et al.*[105] proposed a P2D electrochemical–0D thermal-degradation coupled model, which includes the side reactions on anode and the loss of active material of cathode caused by mechanical stress. However, due to the model complexity, the electrical–thermal–degradation coupled model is usually hard to use in online applications. Even for the battery design application, the computational cost seems still too high. Therefore, how to reduce the model complexity and develop the effective model reduction methods needs to be further explored.

The simulation of multi-physics coupled models is more complicated. Except for the lumped parameters ECM–0D thermal model that can be easily solved discretely, almost all other coupled models contain complex PDEs. Hence, the numerical calculation methods such as FDM, FEM, and FVM are usually adopted. Besides, for the coupled models that are composed of sub-models with different dimensions, the volume-average strategy is usually adopted to realize the parameters transfer between different sub-models.

2.3. Parameters identification

Parameters identification is a vital step for constructing the battery model. In a battery model, only a few parameters can be measured directly, while others need to be estimated based on experimental data, e.g., measured current–voltage response profiles or current–voltage–temperature response profiles. Hence, it is essential to properly carry out experiments to obtain data for parameter estimation. A generalized electrical and thermal parameter estimation problem can be formed as the following weighted least-square optimization problem:

$$\begin{aligned}\min\ \text{obj} = &\left(w_1 \sum_{i=1}^{N} \left(U_{\text{exp},i} - U_{\text{sim},i}(\boldsymbol{x},\boldsymbol{y}) \right)^2 \right. \\ &\left. + w_2 \sum_{i=1}^{N} \left(T_{\text{exp},i} - T_{\text{sim},i}(\boldsymbol{x},\boldsymbol{y}) \right)^2 \right), \end{aligned} \tag{5}$$

subject to

$$\begin{aligned} &h(\boldsymbol{x},\boldsymbol{y}) = 0, \\ &g(\boldsymbol{x},\boldsymbol{y}) \leqslant 0, \\ &\boldsymbol{x} \in [\boldsymbol{x}_{\min}, \boldsymbol{x}_{\max}], \\ &\boldsymbol{y} \text{ is integer}, \end{aligned} \tag{6}$$

where $\boldsymbol{x}$ is the model parameters; $\boldsymbol{y}$ is the model structure parameters; U_{exp} and T_{exp} are the experimental voltage and temperature data, respectively; U_{sim} and T_{sim} are the simulated voltage and temperature, respectively; w_1 and w_2 are defined to adjust the weights of voltage error and temperature error, respectively; $h(\boldsymbol{x})$ is the equations of equality constraints, which is often related to the battery model; and $g(\boldsymbol{x})$ is the equations of inequality constraints. In general, the parameter identification problem of battery model is essentially a nonlinear programming (NLP) problem. In most cases, it is treated as a single-objective optimization problem, which aims to minimize the terminal voltage or temperature difference between the simulated and experimental results. However, if the electrical and thermal parameters need to be identified simultaneously, the optimization problem might be formulated as a multi-objective problem.[73] Moreover, when the function form which describes the relationship between parameters and battery states is variable, the simultaneous optimization problem of the function structure $\boldsymbol{y}$ and parameters $\boldsymbol{x}$ would arise, which can be formulated as a mixed-integer nonlinear programming (MINLP) problem.[106]

In practical application, the parameter identification procedure is usually different according to the different battery model type. For the ECM model, the OCV–SOC relationship is usually modeled by a predefined analytical function and the OCV model parameters could be independently estimated by OCV–SOC experimental data.[107] Other state dependent circuit parameters in the ECM model, e.g., ohmic resistance,

charge transfer resistance, and capacitance, are usually estimated by the charge/discharge current–voltage response profiles. Both one- and two-step approaches have been utilized to the circuit parameters estimation. In the two-step approach, the circuit parameters are first estimated one-by-one from the pulse charge/discharge current–voltage response profiles at different SOC values and then the circuit parameters look-up table is established with respect to SOC. The circuit parameters at unseen SOC are obtained by the interpolation method. Another way is to construct analytical functions, e.g., polynomial or exponential function, by means of the circuit parameters and SOC data in look-up tables.[108–110] In the one-step approach, the coefficients of the predefined functions for state dependent circuit parameters are directly estimated by fitting the current–voltage response profiles over a whole SOC range. Although the parameter estimation optimization problem in the one-step approach is much more complex, the established model is usually more accurate and stable.

The number of parameters in the electrochemical model is much larger than that of parameters in the ECM, making the parameter estimation process more difficult. Different optimization algorithms have been adopted for the optimal parameter identification of the electrochemical model, such as genetic algorithm,[28,73] particle swarm algorithm,[111] and heuristic algorithm.[112] Experiments based on half-cells are usually conducted for the essential model information such as the OCV–SOC relationship at each electrode. Even though the parameter identification based on the half-cell testing can reduce the number of model parameters, how to obtain a global optimal solution is still difficult as there exhibits multiple local optima in the parameter optimization problem. In addition, during the solution process of the parameter optimization problem, the time-consuming electrochemical model needs to be simulated repeatedly. Therefore, the efficient global optimization algorithm should be paid more attention in future.

When identify the thermal parameters in a multi-physics electrical–thermal coupled model, there are usually two ways. One way is to use the experimental data from various thermal property tests such as accelerating rate calorimeter,[113] thermal impedance spectroscopy,[114] and heat flow calorimeter.[115] Another way is to estimate according to the temperature evolution profiles based on a thermal model.[73] Although the thermal parameters might vary with the battery states such as SOC,[116,117] temperature,[118] and aging,[119] the effects of battery state on thermal parameters are usually ignored in the electrical–thermal coupled model. It should be noted that the effective estimation of the aging dependent thermal parameters is still a challenging task and needs to be further explored.

3. Optimal design methodology of LIBs

Optimal tuning design parameters of LIBs is important to the battery performance improvement. At present, the most common way is the trial and error method, which optimizes the design parameters based on the iterative experiments. It is intuitive, but high experimental cost and time consuming. Alternatively, the computer aided design method is more efficient. By resorting to the accurate mathematical models and efficient simulation methods, the optimization algorithms can tune the design parameters of LIBs with respect to different optimization objectives. It is worth noting that, to meet different application requirements, the optimal design of LIBs usually needs to balance between the different battery performance criteria, e.g., energy density, power density, service life, and safety. Moreover, to meet the different design requirements, the battery model type needs to be selected properly according to the design scale, i.e., electrode, cell, and pack. For example, the P2D electrochemical model can be used to study the effects of electrode thickness and porosity on battery specific energy and specific power. A 3D electrical–thermal coupled model can be used to study the effects of cell size, tab size, and position on the electrical and thermal consistency, as well as the specific energy and power. In some cases, a battery module model could be used for the optimal design of thermal management system. To conclude, the model based optimal design strategy can not only improve the battery overall performance, but also greatly reduce the battery design time and cost.

3.1. Design on electrode scale

In general, the parameters on electrode scale mainly contain the thickness and porosity of positive and negative electrodes, and the particle size distribution. The optimization of the electrode scale parameters is usually conducted based on the P2D based model. In the ECM, the electrode scale parameters are not considered, while in the SP model, the non-uniformity in the thickness direction is neglected, which make them seldom used in the electrode scale parameter optimization. According to the various requirements on the battery performance improvement, the optimization parameters of electrode scale mainly include electrode thickness,[120–122] electrode porosity,[123] positive and negative electrode capacity ratio,[124] and particle size.[125]

To maximize the specific energy or discharge capacity, some works proposed to optimize the electrode thickness and porosity based on the P2D model. Srinivasan *et al.*[126] carried out the optimization of the electrode thickness and porosity of graphite/$LiFePO_4$ battery, which achieved maximum specific energy at given discharge time (from 10 h to 2 min). In this study, the porosity of the negative electrode remained constant while the thickness of the negative electrode was

changed according to the ratio of the positive and negative active materials. The similar strategy was adopted by Appiah *et al.*[127] to optimize the electrode thickness and porosity of graphite/$LiNi_{0.6}Co_{0.2}Mn_{0.2}O_2$ battery, in which the P2D model was modified to include the effect of contact internal resistance difference. De *et al.*[128] proposed a multi-step optimization approach to optimize the electrode thickness and porosity of both electrodes, in which the optimization variables were added one by one during the optimization procedure. Dai *et al.*[129] maximized the energy density of the battery by optimizing the porosity of the positive and negative active materials and the thickness of the positive electrode, meanwhile a direct search method was adopted for optimization. The results of graded electrode porosity design were then compared with the results of uniform porosity design.

When conducting the particle size optimization, the P2D model must include the stress and the side reaction effects, otherwise the particle size of the active materials would favor to be as small as possible for decreasing the solid diffusion polarization. Golmon *et al.*[130] combined the P2D model with a mechanical model to simulate the stress introduced by lithium diffusion, in which the stress level was bounded by a maximum value to control the capacity fading rate. In this study, the local porosity and local particle radii at each finite element node of both electrodes greatly increased the optimization variables, hence, the globally convergent method of moving asymptotes of Svanberg was adopted to handle the complex optimization problems. Liu *et al.*[131] used an P2D electrochemical–degradation coupled model to simultaneously maximize specific energy and specific power and minimize the capacity loss with respect to electrode thickness, electrode porosity, and particle size. The elitist non-dominated sorting genetic algorithm (NSGA-II) was adopted to solve the multi-objective optimization problem.

For large format batteries, the effects of electrode scale parameters on battery thermal performance are usually taken into account. Zhao *et al.*[75] studied the effects of electrode thickness on battery performance using P2D elelctrochemcial–3D thermal model. Mei *et al.*[76] studied the effects of electrode thickness, electrode porosity, and particle size on battery electrochemical and thermal performance. In addition, some studies have focused on designing structured electrode using electrochemical model. Cobb *et al.*[132,133] proposed co-extruded electrode structures to improve the battery energy density, and simulation study was taken using a dimension-extended P2D model. Nemani *et al.*[134] proposed a bi-tortuous, anisotropic graphite anodes structure to improve the ion transportation, and the equations of the P2D model were extended to 2D to carry out the simulation. However, the industrial production of such structured electrode remains quite difficult. In general, given predefined current profile, most optimal design problems on electrode scale can be formulated as single objective optimization problems with respect to maximize the specific energy or discharge capacity. If the charge/discharge current is considered to be an additional optimization variable, multiple objectives need to be simultaneously optimized for balancing the tradeoff between specific energy and specific power.[135]

3.2. Design on cell scale

The design parameters on cell scale mainly refer to electrode size, tab size and location, number of stacks, etc. Usually, with the scale up of battery size, the non-uniformity of both electrical and thermal distributions will become more severe, and then the battery charge/discharge performance and service life will deteriorate significantly.[136,137] Hence, the design strategy on the cell scale is quite important, especially for large format batteries.

In general, both 2D and 3D models can be employed for the optimization of cell scale parameters. Based on the ECM–thermal coupled model, Kim *et al.*[138] studied the effects of the electrode size and tab location on the potential, current density, and temperature distributions with a 2D electrical–thermal coupled model. Kosch *et al.*[139] studied the effects of tab location and size on the temperature distribution of a pouch type cell using a 2D ECM–thermal coupled model. A 2D ECM–3D thermal coupled model was proposed by Wu *et al.*[67] and used for the thermal design of pouch cell,[140] in which the temperature distributions of cells with different electrode sizes and different tab locations were systematically compared.

Also, there have been studies about the optimization of cell scale parameters based on the electrochemical model. Mei *et al.*[141] used a P2D electrochemical–3D thermal model to study the effects of tab dimension on the thermal performance of pouch type cell. Zhang *et al.*[142] studied the impacts of tab locations and electrode size on the temperature distribution of pouch type cell, in which the uniformity of temperature distribution under different design configurations was studied by a P2D electrochemical–2D thermal coupled model. Samba *et al.*[30] studied the influence of the position of the tab on the current density, voltage, and temperature distribution by establishing a 3D electrochemical–3D thermal coupled model for a pouch cell with single electrode plate pair. Rieger *et al.*[29] used a 3D electrochemical–2D thermal–2D stress coupled model to study the effects of tab position on the battery performance, except for the uniformity of temperature and current density distribution, the mechanical criteria were also introduced for rating different designs.

It is found that the optimization of design parameters on cell scale is usually realized by parametric studies, while the optimization algorithms are seldom explicitly used to perform

design optimization. The main reason is that the simulation of 2D or 3D coupled model used on cell scale is time-consuming, which hinders the direct application of the optimization algorithm to some extent. In addition, the simultaneous consideration of multiple performance criteria such as energy density, service life, uniformity, and cost would further increase the optimization difficulty greatly. Hence, more efficient global optimization algorithms are expected for such complex multi-objective battery design optimization problems.

3.3. Design on pack scale

A battery pack usually consists of dozens even hundreds of cells, which makes the thermal issues increasingly prominent. To guarantee the safe operation and extend battery life, the battery pack should be carefully designed not only to avoid local heat accumulation but also to improve the temperature consistency among cells. On the pack scale design optimization, both cell arrangement and cooling strategy usually need to be simultaneously optimized. In general, a simple electrical–thermal coupled model,[143] or even empirical thermal model,[144] is used to simulate the cell heat generation characteristics. By the combination of such simple thermal models with computational fluid dynamics simulation, the gap spacing between cell, the flow speed of air or liquid can be optimized to achieve uniform temperature distribution and lower maximum temperature rise. Although these simplified battery models are helpful to reduce the computational complexity, their generalization ability and the effectiveness of optimal pack design schemes need to be further verified.

Besides, more precise battery models have been introduced to assist in the optimal design on the pack scale. Tong *et al.*[145] studied the effects of operational and design parameters on the pack performance using liquid cooling strategy, in which the internal physical property distribution of each battery was simulated with an electrochemical–thermal coupled model. Based on that, an electrochemical–thermal coupled model combined with 2D thermal–fluid conjugate model was proposed to study the effects of different cell arrangements on the temperature distribution in a battery module.[146] A 2D electrochemical–2D thermal coupled model was used by Bandhauer *et al.*[147] to study different cell designs (8 A·h and 20 A·h) and cooling strategies on the temperature and current distributions during dynamic loads operation. Darcovich *et al.*[148] compared different cooling plate configurations of battery pack, in which an SP electrochemical–3D thermal model was used to simulate the battery performance. An air cooling strategy for battery pack was developed by Sun *et al.*[149] based on a 3D battery module thermal model, in which each cell was simulated using an ECM–3D thermal coupled model. The similar model was also used to develop a liquid cooling system for a battery module,[150] moreover, an analytical optimization approach was developed for the identification of optimal design concept. Zhao *et al.*[151] studied the effects of different cooling strategies on the temperature rise and gradient of a pouch cell using a 2D ECM–2D thermal coupled model, in which both surface and tab cooling strategies were compared.

Table 1. Summary of model based battery design methods on electrode, cell, and pack scales.

Scale	Model type	Design variable	Design objective	Methods and reference
Electrode	P2D	Electrode thickness and porosity	Specific energy; Specific power;	Parametric study[126,127] Optimization[128,129]
	P2D-stress/P2D-degradation	Electrode thickness and porosity Particle size	Specific energy; Specific power; Stress	Optimization[130,131]
	P2D-thermal	Electrode thickness; Electrode porosity	Specific energy; Specific power; Temperature distribution; Maximum temperature;	Parametric study[75] Optimization[76]
Cell	ECM-thermal	Electrode size; Tab location; Tab size	Potential, current, Temperature, SOC distributions.	Parametric study.[138–140]
	Electrochemical-thermal	Electrode size; Tab location; Tab size	Potential, current, Temperature, SOC distributions.	Parametric study[30,141,142]
	Electrochemical-thermal combined with stress	Electrode size; Tab location; Tab size	Potential, current, Temperature, SOC distributions.	Parametric study[29]
Pack	ECM-thermal	cell arrangement related parameters; cooling strategy related parameters;	Maximum temperature; Temperature distribution;	Parametric study[143,145–148,151]
	Electrochemical-thermal	cell arrangement related parameters; cooling strategy related parameters;	Maximum temperature; Temperature distribution;	Parametric study[149] Optimization[150]

The application of more accurate battery model is expected to increase the effectiveness and reliability of the battery pack design. However, the introduction of accurate battery would significantly increase the model complexity on the pack scale and consequently might result in very high simulation computational cost, especially combined with optimization algorithms. To tackle this issue, the advanced modeling strategies, which possess high accuracy and high efficiency, are expected to be developed. Moreover, with the intend of reducing the computational cost, the coupling strategies between

the cell scale and pack scale requires more attention. In addition, like the design on the cell scale, the multi-objective optimization method on the pack scale needs to be further studied. The references in battery design on different scales are summarized in Table 1, in which the methods are classified based on the adopted battery model.

4. Management method of LIBs

Each type of LIBs has its own safe operating area (SOA), including but not limited to the operating voltage window, operating temperature, and operating current.[152] Once the operation conditions exceed the SOA, the LIBs are prone to undergo the irreversible damage even safety accident. It should be pointed out that these constraints are not simple box constraints, and some constraints are highly dependent on the state of the battery. For example, the trigger temperature of the thermal runaway is related to the SOC of the battery, while the limit of charge current lies on the battery temperature. For a complex battery system, the single cell safety is the basis of the whole system. Therefore, ensuring each cell operating within its SOA is the critical requirement of BMS on various scales.

During the battery operation, the battery states, such as SOC, state of health (SOH), state of power (SOP), and internal temperature, need to be monitored in real time.[153] These battery states not only are necessary information to users, but also help to improve the battery management efficiency, which makes them become the cores of BMS. However, suffering from the nonlinear dynamic characteristics and the aging behavior under long-term cycling, accurate battery state estimation is usually difficult. To solve this problem, various model-based state estimation algorithms have been proposed, and become the key research issues in BMS.[154]

In this paper, the state estimation and internal temperature monitoring methods will be discussed in details. Other issues such as equalization,[155,156] safety management,[157–159] thermal management,[13,16] and fault diagnosis[160] are not covered, as some of them are realized by model-free methods and some functions are comprehensively reviewed in existing literatures.[153]

4.1. SOC estimation

As illustrated by Li *et al.*,[161] the SOC of battery could be defined from different perspectives. From the thermodynamics perspective, the SOC describes the lithium ion concentration in an electrode or in two electrodes of a single cell. From the engineering perspective, the SOC is used to describe the remaining useful capacity of battery, which can be defined as

$$\mathrm{SOC} = \frac{Q_{\mathrm{res}}}{Q_{\mathrm{max}}}, \tag{7}$$

where Q_{res} is the remaining useful capacity, and Q_{max} is the maximum capacity.

The A·h-counting method is the simplest way for SOC determination. With the measured current and known initial SOC, the SOC at any moment can be calculated by

$$\mathrm{SOC}(t) = \mathrm{SOC}_0 - \frac{\int_0^t \eta I \mathrm{d}t}{Q_{\mathrm{max}}}, \tag{8}$$

where SOC_0 is the initial SOC, η is the coulombic efficiency, and I is the measured current.

Although the A·h-counting method is easily implemented, it has several defects. First, the current measurement noise integrates during the iteration process. Second, the battery capacity fades with aging cannot be corrected. Moreover, the accurate initial SOC is hard to obtain in real applications. Although some works proposed the SOC–OCV relationship to improve the initial SOC accuracy, this method is only available under long-term standing conditions. Furthermore, for the batteries with very flat OCV curve like $LiFePO_4$, the SOC estimation from SOC–OCV relationship may also have great errors. Some other specific operation conditions can also be used for SOC calibration, for example, when the battery is charged or discharged to preset cut-off certification conditions, the SOC can be determined as 100% and 0%, respectively. It should be pointed out that, the calibration methods mentioned above face the risk of failure, because the application scenarios of the battery and the usage habits of specific users vary widely.

To solve this problem, the model-based SOC estimation methods have been developed, which are the combinations of battery model and state estimation algorithms. Figure 3 gives a general framework of model based battery SOC estimation methods. During battery state estimation, a battery model is used to predict the battery terminal voltage. The model predicted terminal voltage is then compared with the measured value, the errors are then taken as the input of the estimation algorithms. The obtained battery SOC is used to update the input of the battery model and sate equation.

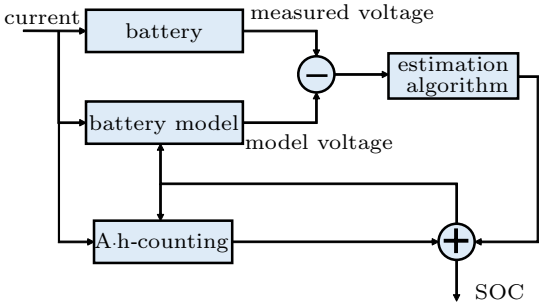


Fig. 3. General flow chart of model based battery SOC estimation method.

The ECM model and SP model are two main model types for SOC estimation. Based on ECM, different estimators have been constructed by adopting different estimation algorithms. The mostly used one is the Kalman filter (KF)

family, including extended Kalman filter (EKF),[162–164] unscented Kalman filter (UKF),[165,166] and sigma-point Kalman filter (SPKF).[167,168] Other methods such as particle filter (PF),[169] sliding mode observer,[170] H-infinity observer,[171] proportional-integral observer,[172] Luenberger observer,[173] moving horizon estimation (MHE)[174,175] combined with ECM for SOC estimation have also been developed. Based on the SP model, the EKF,[176,177] UKF,[178] PF,[179] Luenberger observer,[180,181] adaptive PDE observer[182] based estimators were studied. In addition, some researchers have tried to use the combination of P2D model and KF based algorithms to realize the SOC estimation.[183–185] Although the KF based estimator has proven the good performance, it still has several challenges in real applications. First, the noise covariances are difficult to determine. The unsuitable choice of noise covariances would not only reduce the estimation accuracy, but also result in the risk divergence. Moreover, the hard constrains cannot be added to the algorithms directly. Hence, adaptive EKF (AEKF),[186] adaptive UKF (AUKF),[187] and adaptive PF (APF)[188] have been proposed to update the noise covariances matrix.

To improve the SOC estimation accuracy under wide operation temperature region, different methods have been proposed to integrate the effect of temperature on parameters. One method is to adopt a temperature-compensated model, in which the temperature is measured and treated as an input to correct the model parameters. From this view, the combinations of temperature-compensated ECMs and EKF,[189] UKF,[190] PF,[191] the combination of temperature-compensated SP models and Luenberger observer,[86] are proposed successively. Another method is to adopt an electrical–thermal coupled model, in which the temperature and SOC are estimated simultaneously during the SOC estimation. Following this way, Bizeray *et al.*[70] proposed an P2D electrochemical–thermal coupled model and EKF based battery state estimation method. Notice that the time-step of EKF was set as 5 s to reduce the computation time.

Table 2 compares different SOC estimation methods, in which the advantages and disadvantages are compared between A·h-counting method, OCV based method, and model based methods. Numerous model based SOC estimation methods have been proposed over the past decades. However, it is hard to determine which one is most suitable for real applications. Since the evaluation of SOC estimation methods is multi-dimensional, containing the computational complexity, estimation accuracy, and robustness, more comparative studies need to carry out.[192–196] From the perspective of model, it is widely recognized that although the P2D model is most accurate, it is too complex to implement in the real-time applications. By contrary, the ECM is much simpler and can meet the usual accuracy requirement. This makes it widely accepted by researchers from different fields. The SP model provides a compromise between the accuracy and the complexity, and shows a good estimation stability in the long-term.

Table 2. Comparison between different SOC estimation methods.

Method	Advantage	Disadvantages
A·h-counting	Easy to implement.	Accuracy depends on the initial SOC value. Fault with long term current measurement accumulative error. Self-discharge rate, coulomb efficiency needed.
OCV based	Easy to implement.	Long rest time required. Fault when OCV-SOC curve is flat.
Model based	Initial SOC value insensitive. No rest time needed.	More efforts on the modeling and estimator design. Software demand increasing.

4.2. SOH estimation

SOH is an indicator for battery aging state, which can be defined by capacity fading and internal resistance increasing. The following equations give respectively the definition of SOH by battery capacity and internal resistance:

$$\mathrm{SOH} = \frac{\mathrm{Cap}(t)}{\mathrm{Cap}_{\mathrm{new}}}, \tag{9}$$

$$\mathrm{SOH} = \frac{R_{\mathrm{end}} - R_{\mathrm{int}}(t)}{R_{\mathrm{end}} - R_{\mathrm{new}}}, \tag{10}$$

where $\mathrm{Cap}_{\mathrm{new}}$ is the capacity of a new battery; $\mathrm{Cap}(t)$ is the battery capacity at time t; R_{end} is the internal resistance when the battery reaches the end of life; R_{new} is the internal resistance when the battery is fresh; and $R_{\mathrm{int}}(t)$ is the battery internal resistance at time t.

In the past decades, different model-free methods have been proposed for the SOH estimation, herein, model refers specifically to the model described in Section 2. In some works, the capacity loss or the capacity serves as the SOH indicator, which is presented as a function of time and operation conditions such as current, temperature, DOD, and cycle number.[197–199] Besides that, some researchers used the feature extraction based on battery charge/discharge curve to obtain the battery capacity.[200–203] Since the operation conditions of battery are quite unpredictable, this method is limited for the on-line usage.

Model based SOH estimation method is regarded as an effective way to enhance the estimation accuracy. When the internal resistance serves as the SOH indicator, the EIS based SOH estimation methods are widely studied. By establishing the frequency-domain ECM, the internal resistance associated with internal reaction and transfer phenomena can be identi-

fied, and then the SOH can be evaluated.[204] Because of the high cost of test equipment,[205] the difficulty of excluding the effects of SOC and temperature on internal resistance, the implementation of EIS for on-line usage is still challenging.

Either use the capacity or the internal resistance as the SOH indicator, the alternative way for the SOH estimation is the combination of battery model and observer/filtering algorithms. Usually, joint or dual estimation techniques are adopted, which can obtain the estimation of SOC and SOH simultaneously.[206] Figure 4 compares the general frameworks of joint and dual estimators for SOC and SOH. In a joint estimation approach, a single sate vector is used for both parameters and state estimation. The internal resistance or capacity, as an indicator of SOH, is added in the state equation. Then both SOC and SOH are estimated simultaneously in each iteration. While in a dual estimation approach, two estimators are used in parallel, one is used for the SOC estimation and the other one is used for the SOH estimation.

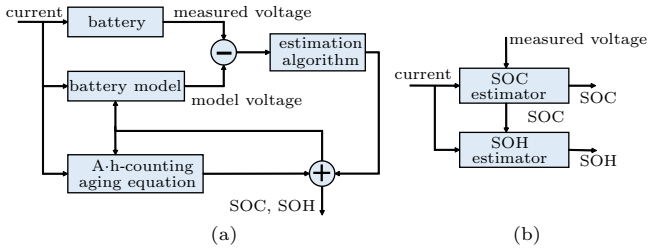


Fig. 4. Comparison of joint and dual estimation methods for SOC and SOH: (a) joint estimation method; (b) dual estimation method.

Based on ECM, the EKF,[207,208] least squares estimation,[209] PF,[210] dual sliding mode observer[211] for SOH estimation have been proposed. Notice that, unlike SOC, SOH usually varies slowly during the operation, therefor, the battery SOH can be estimated on a longer time scale. Combined estimation methods such as two EKF,[212] EKF combined with recursive least squares[213,214] have also been developed. Based on the SP model, the SOH estimation is realized using PF,[215] least squares method,[216] sliding mode observers,[217] adaptive output-injection observer,[218] adaptive PDE observer,[182] and trinal proportional-integral observers.[219]

4.3. SOP estimation

SOP is defined as the maximum power that a battery can deliver or receive on upcoming time scale, generally several seconds, meanwhile, ensuring the safe operation of battery.[220] It is an essential battery state especially for vehicle usage during operations such as acceleration, climbing, or regenerative braking. SOP depends on many other battery states such as SOC, temperature, and SOH. Therefore, the SOP estimation performance is strongly affected by the accuracy of the SOC, temperature, and SOH estimation.[221]

A direct way to obtain SOP is to establish the relationship of SOP with SOC, temperature, and SOH. Generally, the empirical function or look-up table is first constructed off-line based on the pre-designed laboratory tests. Then, the SOP estimation is conducted by bringing the online measurement data into the preset equation or look-up table. This method is simple and easy to implement. However, since the effect of the load history is neglected, there might be great estimation errors in real applications.[222]

Model-based method is an effective way to improve the estimation accuracy of SOP. Based on ECM,[220,223,224] ECM–thermal coupled model,[225,226] and SP model,[227] various SOP estimation methods have been proposed and compared in details.[228] In these methods, the battery model is used to obtain the maximum power capability such that the SOC and the simulated voltage are kept within the preset region, meanwhile, temperature constrains are satisfied based on a thermal model.[226] In order to reduce the calculation complexity and meet the real-time requirement, battery models have to be simplified, which might introduce the errors into the estimation process. Therefore, how to choose a proper model complexity is critical in the real applications. When conducting the SOP estimation, the boundary method is most widely used, which is directly based on the design boundaries and the operation boundaries. Besides that, considering the nonlinear properties of the battery model, the SOP estimation can also be treated as an optimization problem, where the objective is the maximum battery power within the preset time region, and the constraints are the allowed SOC, voltage, and temperature. By solving this problem, the SOP estimates could be obtained effectively. Although the adoption of optimization algorithms such as Karush–Kuhn–Tucker (KKT) conditions[229] and genetic algorithm[230] allows more accurate estimation, its computational cost is higher when compared to the traditional methods.

4.4. Internal temperature estimation

In most existing BMS, the battery temperature is directly determined by the sensor measurement at battery surface. However, in practice, the battery internal temperature could greatly differ from the surface temperature, especially under extreme operation conditions such as large current rate.[231,232] It means that even the surface temperature is within the allowed region, the unexpected reactions still possibly happen inside due to the high internal temperature. Hence, to extend battery life and reduce thermal safety risks, it needs to monitor the internal temperature in real-time.

To realize the real-time monitoring of battery internal temperature, some researchers tried to use embedded thermocouples or fiber sensors to obtain the internal temperature directly.[233,234] Although it is intuitive, the installation of thermocouples and fiber sensors is difficult during the assembly

process and would affect the battery performance. Alternatively, some non-intrusive methods like EIS[235,236] have been used, however, they are restricted in the practical application because of the complicated test procedure and the expensive equipment. The model-based method provides another way to get an accurate estimation of the internal temperature. Lin *et al.*[237] proposed an adaptive observer for the core temperature estimation based on a two-state lumped parameter thermal model, in which the reversible heat generation and SOC dependence of internal resistance were neglected. Zhang *et al.*[238] proposed a KF based internal temperature estimation method, in which a simplified ECM–thermal coupled model was used while the SOC effects on the ECM parameters were neglected. The similar thermal model was also adopted and combined with KF by Sun *et al.*[239] Kim *et al.*[240] proposed a 1D thermal model and dual KF based method for internal temperature monitoring, in which polynomial approximation was used for the thermal model reduction. Dai *et al.*[241] proposed an equivalent electrical network thermal model combined with adaptive KF approach for the internal temperature estimation. In these works, the SOC is an essential parameter for a model based internal temperature estimator, because both reversible and irreversible heat generation rates are calculated based on it. Table 3 summaries the applications of battery models in battery state estimation.

Table 3. Summary of battery state estimation methods used in literature.

State	Models adopted	Methods and references
SOC	ECM based model	EKF,[162–164] UKF,[165,166] SPKF,[167,168] PF,[169] Sliding mode observer,[170] H-infinity observer,[171] Proportional-integral observer,[172] Luenberger observer,[173] MHE,[174,175] AEKF,[186] AUKF,[187] APF[188]
	SP based model	EKF,[176,177] UKF,[178] PF,[179] Luenberger observer,[86,180,181] Adaptive PDE observer[182]
	P2D based model	Linear KF,[183] EKF,[70] PF,[184] output error injection observer[185]
SOH	ECM based model	EKF,[207,208] least squares estimation,[209] PF,[210] dual sliding mode observer,[211] two EKF,[212] EKF with recursive least squares[213,214]
	SP based model	PF,[215] LS,[216] sliding mode observer,[217] adaptive output-injection observer,[218] adaptive PDE observer,[182] trinal proportional-integral observers[219]
SOP	ECM based model	Constraints based calculation,[220,223–226] Optimization based estimation[229,230]
	SP based model	SP model[227]
Internal temperature	ECM-thermal	Adaptive observer,[237] KF,[238,239] Dual KF,[240] Adaptive KF[241]

5. Conclusion

The implementation of the process systems engineering concept is an effective way to accelerate the optimal design process and realize the optimal management of LIBs. In this paper, different kinds of battery models, simulation approaches, and optimization methods are reviewed with a focus on their applications in battery design and management. For this, scientific and technical literatures are studied and all approaches are classified in various groups.

Different LIB models have been developed over the past decades. They differ significantly in the basic principle, model accuracy, and model complexity. However, most of the proposed methods have been developed for the new batteries. It is necessary to extend these models to be suitable for dealing with aged batteries.

Both derivate-based and derivate-free optimization methods have been applied to the various application areas of LIBs, e.g., parameter estimation, battery design, and battery management. However, these methods without proper design might not guarantee the optimization stability and efficiency. Therefore, more attention should be paid to the development of more specific optimization methods, which can ensure their robustness and efficiency in the model parameter estimation, design optimization, and management for LIBs.

Most of the developed optimal design methods for LIBs are based on the battery models. Due to the high model complexity, performing model based optimal battery design is usually time consuming. Therefore, how to achieve the tradeoff between model complexity and model accuracy is crucial to the efficient implementation of design optimization. Although the electrochemical based multi-physics coupled model has proven a possibility of battery design parameter optimization in one optimization procedure, only few related studies have been conducted. In addition, not only the quantitative battery performance criteria but also the relationship among quantitative criteria need to be further proposed and studied.

Although model-based state estimation methods have been widely developed in the past decades, most methods are only focused on handling one state or two states estimation issues. With the higher requirement of BMS, the joint estimation algorithms for multiple states, such as SOC, SOH, SOP, and internal temperature in one integrated framework are worthy of further exploration and development in the future.

To conclude, various advanced modeling, simulation, and optimization methods have been developed for optimal design and management of LIBs during the last decades. However, successful applications of these advanced approaches to practical battery industry are rarely reported. Hence, further studies should be focused on the development of proper solution

approach to satisfy the practical application requirements. In addition, it is worth noting that the development of a software platform with integrated modeling, simulation, and optimization methods of LIBs could be greatly helpful to accelerate the advanced techniques to practical industrial applications of LIBs.

References

[1] Chen H Q, Wang X, He L, Chen P, Wan Y, Yang L and Jiang S 2016 *Renew. Sust. Energ. Rev.* **58** 966
[2] Song J, Yan W, Cao H, Song Q, Ding H, Lv Z, Zhang Y and Sun Z 2019 *J. Clean. Prod.* **215** 570
[3] Yoshino A 2012 *Angew. Chem. Int. Ed.* **51** 5798
[4] Soloveichik G L 2011 *Annu. Rev. Chem. Biomol. Eng.* **2** 503
[5] Blomgren G E 2017 *J. Electrochem. Soc.* **164** A5019
[6] Grossmann I E and Harjunkoski I 2019 *Comput. Chem. Eng.* **126** 474
[7] Shen M and Gao Q 2019 *Int. J. Energy Res.* **43** 5042
[8] Fotouhi A, Auger D J, Propp K, Longo S and Wild M 2016 *Renew. Sust. Energ. Rev.* **56** 1008
[9] Seaman A, Dao T S and McPhee J 2014 *J. Power Sources* **256** 410
[10] Nejad S, Gladwin D T and Stone D A 2016 *J. Power Sources* **316** 183
[11] Doyle M, Fuller T and Newman J 1993 *J. Electrochem. Soc.* **140** 1526
[12] Shrivastava P, Soon T K, Idris M Y I B and Mekhilef S 2019 *Renew. Sust. Energ. Rev.* **113** 109233
[13] Bandhauer T M, Garimella S and Fuller T F 2011 *J. Electrochem. Soc.* **158** R1
[14] Gao T, Wang Z, Chen S and Guo L 2019 *Int. J. Heat Mass Transf.* **141** 419
[15] Guo L S, Wang Z R, Wang J H, Luo Q K and Liu J J 2017 *J. Loss Prev. Process Ind.* **49** 953
[16] Wang Q, Jiang B, Li B and Yan Y 2016 *Renew. Sust. Energ. Rev.* **64** 106
[17] Broussely M, Biensan P, Bonhomme F, Blanchard P, Herreyre S, Nechev K and Staniewicz R J 2005 *J. Power Sources* **146** 90
[18] Doyle M, Newman J and Fuller T F 1994 *J. Electrochem. Soc.* **141** 982
[19] Wang B, Li S E, Peng H and Liu Z 2015 *J. Power Sources* **293** 151
[20] Illig J, Ender M, Chrobak T, Schmidt J P, Klotz D and Ivers-Tiffée E 2012 *J. Electrochem. Soc.* **159** A952
[21] Buller S, Thele M, De Doncker R W A A and Karden E 2005 *IEEE Trans. Ind. Appl.* **41** 742
[22] Dong T K, Kirchev A, Mattera F, Kowal J and Bultel Y 2011 *J. Electrochem. Soc.* **158** A326
[23] Xu J, Mi C C, Cao B and Cao J 2013 *J. Power Sources* **233** 277
[24] Mu H, Xiong R, Zheng H, Chang Y and Chen Z 2017 *Appl. Energy* **207** 384
[25] Barai A, Widanage W D, Marco J, McGordon A and Jennings P 2015 *J. Power Sources* **295** 99
[26] Hu X S, Li S B and Peng H 2012 *J. Power Sources* **198** 359
[27] He H, Xiong R and Fan J 2011 *Energies* **4** 582
[28] Forman J C, Moura S J, Stein J L and Fathy H K 2012 *J. Power Sources* **210** 263
[29] Rieger B, Erhard S V, Kosch S, Venator M, Rheinfeld A and Jossen A 2016 *J. Electrochem. Soc.* **163** A3099
[30] Samba A, Omar N, Gualous H, Capron O, Van den Bossche P and Van Mierlo J 2014 *Electrochim. Acta* **147** 319
[31] Jokar A, Rajabloo B, Désilets M and Lacroix M 2016 *J. Power Sources* **327** 44
[32] Santhanagopalan S, Guo Q, Ramadass P and White R E 2006 *J. Power Sources* **156** 620
[33] Zhang D, Popov B N and White R E 2000 *J. Electrochem. Soc.* **147** 831
[34] Kemper P and Kum D 2013 *9th IEEE Vehicle Power and Propulsion Conference*, October 15–18, 2013, Beijing, China, p. 158
[35] Tanim T R, Rahn C D and Wang C Y 2014 *American Control Conference*, June 4–6, 2014, Portland, OR, United States, p. 141
[36] Fuller T F, Doyle M and Newman J 1994 *J. Electrochem. Soc.* **141** 1
[37] Khaleghi Rahimian S, Rayman S and White R E 2013 *J. Power Sources* **224** 180
[38] Ramadesigan V, Northrop P W C, De S, Santhanagopalan S, Braatz R D and Subramanian V R 2012 *J. Electrochem. Soc.* **159** R31
[39] Wang J P, Chen Q S and Cao B G 2006 *Energ. Convers. Manage.* **47** 858
[40] Xu L, Wang J and Chen Q 2012 *Energ. Convers. Manage.* **53** 33
[41] Wang Z, Tong X, Liu K, Shu C M, Jiang F, Luo Q and Wang H 2019 *Fire Mater.* **43** 219
[42] Bernardi D, Pawlikowski E and Newman J 1985 *J. Electrochem. Soc.* **132** 5
[43] Bodenes L, Naturel R, Martinez H, Dedryvère R, Menetrier M, Croguennec L, Pérès J P, Tessier C and Fischer F 2013 *J. Power Sources* **236** 265
[44] Yang L, Takahashi M and Wang B 2006 *Electrochim. Acta* **51** 3228
[45] Li J, Zhang J, Zhang X, Yang C, Xu N and Xia B 2010 *Electrochim. Acta* **55** 927
[46] Li D, Danilov D L, Xie J, Raijmakers L, Gao L, Yang Y and Notten P H L 2016 *Electrochim. Acta* **190** 1124
[47] Bloom I, Cole B W, Sohn J J, Jones S A, Polzin E G, Battaglia V S, Henriksen G L, Motloch C, Richardson R, Unkelhaeuser T, Ingersoll D and Case H L 2001 *J. Power Sources* **101** 238
[48] Hendricks C, Williard N, Mathew S and Pecht M 2015 *J. Power Sources* **297** 113
[49] Arora P, White R E and Doyle M 1998 *J. Electrochem. Soc.* **145** 3647
[50] Zhang Q and White R E 2008 *J. Power Sources* **179** 793
[51] Waldmann T, Hogg B I and Wohlfahrt-Mehrens M 2018 *J. Power Sources* **384** 107
[52] Christensen J and Newman J 2006 *J. Electrochem. Soc.* **153** A1019
[53] Sethuraman V A, Van Winkle N, Abraham D P, Bower A F and Guduru P R 2012 *J. Power Sources* **206** 334
[54] Hu P, Wang B, Xiao D and Aifantis K 2019 *Nano Energy* **63** 103820
[55] Réthoré J, Zheng H, Li H, Li J and Aifantis K E 2018 *J. Power Sources* **400** 383
[56] Kostecki R, Lei J, McLarnon F, Shim J and Striebel K 2006 *J. Electrochem. Soc.* **153** A669
[57] Funayama K, Nakamura T, Kuwata N, Kawamura J, Kawada T and Amezawa K 2015 *Electrochem* **83** 894
[58] Li J, Zhang Q, Xiao X, Cheng Y T, Liang C and Dudney N J 2015 *J. Am. Chem. Soc.* **137** 13732
[59] Samba A, Omar N, Gualous H, Firouz Y, Van Den Bossche P, Van Mierlo J and Boubekeur T I 2014 *Electrochim. Acta* **117** 246
[60] Madani S S, Schaltz E and Kær S K 2019 *Energies* **12** 679
[61] Wang Q K, He Y J, Shen J N, Ma Z F and Zhong G B 2017 *Energy* **138** 118
[62] Du S, Jia M, Cheng Y, Tang Y, Zhang H, Ai L, Zhang K and Lai Y 2015 *Int. J. Therm. Sci.* **89** 327
[63] Kwon K H, Shin C B, Kang T H and Kim C S 2006 *J. Power Sources* **163** 151
[64] Kim U S, Yi J, Shin C B, Han T and Park S 2011 *J. Power Sources* **196** 5115
[65] Kim U S, Yi J, Shin C B, Han T and Park S 2013 *J. Electrochem. Soc.* **160** A990
[66] Goutam S, Nikolian A, Jaguemont J, Smekens J, Omar N, Van Dan Bossche P and Van Mierlo J 2017 *Appl. Therm. Eng.* **126** 796
[67] Wu B, Li Z and Zhang J 2015 *J. Electrochem. Soc.* **162** A181
[68] Rheinfeld A, Kosch S, Erhard S V, Osswald P J, Rieger B and Jossen A 2016 *J. Electrochem. Soc.* **163** A3046
[69] Chacko S and Chung Y M 2012 *J. Power Sources* **213** 296
[70] Bizeray A M, Zhao S, Duncan S R and Howey D A 2015 *J. Power Sources* **296** 400
[71] Northrop P W C, Ramadesigan V, De S and Subramanian V R 2011 *J. Electrochem. Soc.* **158** A1461
[72] Cai L and White R E 2010 *J. Electrochem. Soc.* **157** A1188
[73] Zhang L, Wang L, Hinds G, Lyu C, Zheng J and Li J 2014 *J. Power Sources* **270** 367
[74] An Z, Jia L, Wei L, Dang C and Peng Q 2018 *Appl. Therm. Eng.* **137** 792
[75] Zhao R, Liu J and Gu J 2015 *Appl. Energy* **139** 220
[76] Mei W, Chen H, Sun J and Wang Q 2019 *Sustain. Energy Fuels* **3** 148
[77] Guo M, Kim G H and White R E 2013 *J. Power Sources* **240** 80
[78] Hosseinzadeh E, Genieser R, Worwood D, Barai A, Marco J and Jennings P 2018 *J. Power Sources* **382** 77
[79] Xu M, Zhang Z, Wang X, Jia L and Yang L 2014 *J. Power Sources* **256** 233
[80] Ghalkhani M, Bahiraei F, Nazri G A and Saif M 2017 *Electrochim. Acta* **247** 569

[81] Li H, Liu C, Saini A, Wang Y, Jiang H, Yang T, Chen L, Pan C and Shen H 2019 *J. Power Sources* **438** 226974
[82] Xu M, Zhang Z, Wang X, Jia L and Yang L 2015 *Energy* **80** 303
[83] Allu S, Kalnaus S, Elwasif W, Simunovic S, Turner J A and Pannala S 2014 *J. Power Sources* **246** 876
[84] Guo M, Sikha G and White R E 2011 *J. Electrochem. Soc.* **158** A122
[85] Prada E, Di Domenico D, Creff Y, Bernard J, Sauvant-Moynot V and Huet F 2012 *J. Electrochem. Soc.* **159** A1508
[86] Tanim T R, Rahn C D and Wang C Y 2015 *Energy* **80** 731
[87] Baba N, Yoshida H, Nagaoka M, Okuda C and Kawauchi S 2014 *J. Power Sources* **252** 214
[88] Darcovich K, MacNeil D D, Recoskie S and Kenney B 2018 *Appl. Therm. Eng.* **133** 566
[89] Safari M, Morcrette M, Teyssot A and Delacourt C 2009 *J. Electrochem. Soc.* **156** A145
[90] Lin X, Park J, Liu L, Lee Y, Lu W and Sastry A M 2013 *J. Electrochem. Soc.* **160** A1701
[91] Pinsona M B and Bazant M Z 2013 *J. Electrochem. Soc.* **160** A243
[92] Delacourt C and Safari M 2012 *J. Electrochem. Soc.* **159** A1283
[93] Awarke A, Pischinger S and Ogrzewalla J 2013 *J. Electrochem. Soc.* **160** A172
[94] Lin X, Hao X, Ivanco A, Liu Z and Jia W 2018 *J. Electrochem. Soc.* **165** A2255
[95] Renganathan S, Sikha G, Santhanagopalan S and White R E 2010 *J. Electrochem. Soc.* **157** A155
[96] Li J, Lotfi N, Landers R G and Park J 2017 *J. Electrochem. Soc.* **164** A874
[97] Laresgoiti I, Käbitz S, Ecker M and Sauer D U 2015 *J. Power Sources* **300** 112
[98] Klinsmann M, Rosato D, Kamlah M and McMeeking R M 2016 *J. Electrochem. Soc.* **163** A102
[99] Klinsmann M, Rosato D, Kamlah M and McMeeking R M 2016 *J. Power Sources* **331** 32
[100] Li J, Adewuyi K, Lotfi N, Landers R G and Park J 2017 231*st ECS Meeting*, May 28–June 1, 2017, New Orleans, United States, p. 1003
[101] Li J, Adewuyi K, Lotfi N, Landers R G and Park J 2018 *Appl. Energy* **212** 1178
[102] Deshpande R D and Bernardi D M 2017 *J. Electrochem. Soc.* **164** A461
[103] Xie Y, Li J and Yuan C 2014 *J. Power Sources* **248** 172
[104] Lamorgese A, Mauri R and Tellini B 2018 *J. Energy Storage* **20** 289
[105] Yang S C, Hua Y, Qiao D, Lian Y B, Pan Y W and He Y L 2019 *Electrochim. Acta* **326** 134928
[106] Shen J N, He Y J and Ma Z F 2016 *AIChE J.* **62** 78
[107] He Y J, Shen J N, Shen J F and Ma Z F 2015 *Ind. Eng. Chem. Res.* **54** 3167
[108] Hariharan K S and Kumar V S 2013 *J. Power Sources* **222** 210
[109] Hentunen A, Lehmuspelto T and Suomela J 2014 *IEEE Trans. Energy Convers.* **29** 558
[110] Chen M and Rincón-Mora G A 2006 *IEEE Trans. Energy Convers.* **21** 504
[111] Rahman M A, Anwar S and Izadian A 2016 *J. Power Sources* **307** 86
[112] Li J, Zou L, Tian F, Dong X, Zou Z and Yang H 2016 *J. Electrochem. Soc.* **163** A1646
[113] Vertiz G, Oyarbide M, Macicior H, Miguel O, Cantero I, Fernandez De Arroiabe P and Ulacia I 2014 *J. Power Sources* **272** 476
[114] Fleckenstein M, Fischer S, Bohlen O and Bäker B 2013 *J. Power Sources* **223** 259
[115] Murashko K A, Mityakov A V, Pyrhönen J, Mityakov V Y and Sapozhnikov S S 2014 *J. Power Sources* **271** 48
[116] Bazinski S J and Wang X 2015 *J. Power Sources* **293** 283
[117] Bazinski S J, Wang X, Sangeorzan B P and Guessous L 2016 *Energy* **114** 1085
[118] Loges A, Herberger S, Werner D and Wetzel T 2016 *J. Power Sources* **325** 104
[119] Maleki H, Wang H, Porter W and Hallmark J 2014 *J. Power Sources* **263** 223
[120] Zheng H, Li J, Song X, Liu G and Battaglia V S 2012 *Electrochim. Acta* **71** 258
[121] Suthar B, Northrop P W C, Rife D and Subramanian V R 2015 *J. Electrochem. Soc.* **162** A1708
[122] Yu S, Kim S, Kim T Y, Nam J H and Cho W I 2013 *Bull. Korean Chem. Soc.* **34** 79
[123] Antartis D, Dillon S and Chasiotis I 2015 *J. Compos. Mater.* **49** 1849
[124] Kim C S, Jeong K M, Kim K and Yi C W 2015 *Electrochim. Acta* **155** 431
[125] Jo M, Hong Y S, Choo J and Cho J 2009 *J. Electrochem. Soc.* **156** A430
[126] Srinivasan V and Newman J 2004 *J. Electrochem. Soc.* **151** A1530
[127] Appiah W A, Park J, Song S, Byun S, Ryou M H and Lee Y M 2016 *J. Power Sources* **319** 147
[128] De S, Northrop P W C, Ramadesigan V and Subramanian V R 2013 *J. Power Sources* **227** 161
[129] Dai Y and Srinivasan V 2016 *J. Electrochem. Soc.* **163** A406
[130] Golmon S, Maute K and Dunn M L 2014 *J. Power Sources* **253** 239
[131] Liu C and Liu L 2017 *J. Electrochem. Soc.* **164** E3254
[132] Cobb C L and Blanco M 2014 *J. Power Sources* **249** 357
[133] Cobb C L and Solberg S E 2017 *J. Electrochem. Soc.* **164** A1339
[134] Nemani V P, Harris S J and Smith K C 2015 *J. Electrochem. Soc.* **162** A1415
[135] Du W B, Xue N S, Gupta A, Sastry A M, Martins J R A and Shyy W 2013 *Acta Mech. Sin.* **29** 335
[136] Kim H K, Kim C J, Kim C W and Lee K J 2018 *Comput. Chem. Eng.* **112** 82
[137] Klein M, Tong S and Park J W 2016 *Appl. Energy* **165** 639
[138] Kim U S, Shin C B and Kim C S 2008 *J. Power Sources* **180** 909
[139] Kosch S, Rheinfeld A, Erhard S V and Jossen A 2017 *J. Power Sources* **342** 666
[140] Wu B, Li Z and Zhang J 2014 *Sci. Sin. Tech.* **44** 1154
[141] Mei W, Chen H, Sun J and Wang Q 2018 *Appl. Therm. Eng.* **142** 148
[142] Zhang X, Chang X, Shen Y and Xiang Y 2017 *J. Energy Storage* **11** 249
[143] Chen D, Jiang J, Li X, Wang Z and Zhang W 2016 *Energies* **9** 865
[144] Fan L, Khodadadi J M and Pesaran A A 2013 *J. Power Sources* **238** 301
[145] Tong W, Somasundaram K, Birgersson E, Mujumdar A S and Yap C 2015 *Int. J. Therm. Sci.* **94** 259
[146] Tong W, Somasundaram K, Birgersson E, Mujumdar A S and Yap C 2016 *Appl. Therm. Eng.* **99** 672
[147] Bandhauer T, Garimella S and Fuller T F 2015 *J. Electrochem. Soc.* **162** A125
[148] Darcovich K, MacNeil D D, Recoskie S, Cadic Q and Ilinca F 2019 *Appl. Therm. Eng.* **155** 185
[149] Sun H and Dixon R 2014 *J. Power Sources* **272** 404
[150] Sun H and Dixon R 2016 *J. Electrochem. Soc.* **163** E313
[151] Zhao Y, Patel Y, Zhang T and Offer G J 2018 *J. Electrochem. Soc.* **165** A3169
[152] Waag W, Fleischer C and Sauer D U 2014 *J. Power Sources* **258** 321
[153] Lu L, Han X, Li J, Hua J and Ouyang M 2013 *J. Power Sources* **226** 272
[154] Lin X F, Kim Y, Mohan S, Siegel J B and Stefanopoulou A G 2019 *Annu. Rev. Control Robot. Auton. Syst.* **2** 393
[155] Gallardo-Lozano J, Romero-Cadaval E, Milanes-Montero M I and Guerrero-Martinez M A 2014 *J. Power Sources* **246** 934
[156] Feng F, Hu X, Liu J, Lin X and Liu B 2019 *Renew. Sust. Energ. Rev.* **116** 109464
[157] Abada S, Marlair G, Lecocq A, Petit M, Sauvant-Moynot V and Huet F 2016 *J. Power Sources* **306** 178
[158] Gandoman F H, Jaguemont J, Goutam S, Gopalakrishnan R, Firouz Y, Kalogiannis T, Omar N and Van Mierlo J 2019 *Appl. Energy* **251** 113343
[159] Liao Z, Zhang S, Li K, Zhang G and Habetler T G 2019 *J. Power Sources* **436**
[160] Wu C, Zhu C, Ge Y and Zhao Y 2015 *J. Nanomater.* **2015** 631263
[161] Li Z, Huang J, Liaw B Y and Zhang J 2017 *J. Power Sources* **348** 281
[162] Plett G L 2004 *J. Power Sources* **134** 252
[163] Plett G L 2004 *J. Power Sources* **134** 262
[164] Plett G L 2004 *J. Power Sources* **134** 277
[165] He W, Williard N, Chen C and Pecht M 2013 *Microelectron. Reliab.* **53** 840
[166] Tian Y, Xia B, Sun W, Xu Z and Zheng W 2014 *J. Power Sources* **270** 619
[167] Wang L, Wang L, Liao C and Liu J 2009 5*th IEEE Vehicle Power and Propulsion Conference*, September 7–10, 2009, Dearborn, MI, United States, p. 1592

[168] Li D, Ouyang J, Li H and Wan J 2015 *J. Power Sources* **279** 439
[169] Xia B, Sun Z, Zhang R and Lao Z 2017 *Energies* **10** 457
[170] Kim I S 2006 *J. Power Sources* **163** 584
[171] Zhang F, Liu G, Fang L and Wang H 2012 *IEEE Trans. Ind. Electron.* **59** 1086
[172] Xu J, Mi C C, Cao B, Deng J, Chen Z and Li S 2014 *IEEE Trans. Veh. Technol.* **63** 1614
[173] Yun H, Zhao Y and Zhong Z 2010 *Zhongguo Jixie Gongcheng* **21** 2505 (in Chinese)
[174] Shen J N, He Y J, Ma Z F, Luo H B and Zhang Z F 2016 *Chem. Eng. Sci.* **154** 42
[175] Shen J N, Shen J J, He Y J and Ma Z F 2019 *IEEE Trans. Power Electron.* **34** 4329
[176] Santhanagopalan S and White R E 2006 *J. Power Sources* **161** 1346
[177] Di Domenico D, Stefanopoulou A and Fiengo G 2010 *J. Dyn. Syst. Meas. Control.* **132** 061302
[178] Santhanagopalan S and White R E 2010 *Int. J. Energy Res.* **34** 152
[179] Samadi M F, Alavi S M M and Saif M 2013 *1st American Control Conference*, June 17–19, 2013, Washington, DC, United States, p. 4693
[180] Dey S, Ayalew B and Pisu P 2015 *IEEE Trans. Control. Syst. Technol.* **23** 1935
[181] Lotfi N, Landers R G, Li J and Park J 2017 *IEEE Trans. Control. Syst. Technol.* **25** 1217
[182] Moura S J, Chaturvedi N A and Krstić M 2014 *J. Dyn. Syst. Meas. Control.* **136** 011015
[183] Smith K A, Rahn C D and Wang C Y 2010 *IEEE Trans. Control. Syst. Technol.* **18** 654
[184] Samadi M F, Alavi S M M and Saif M 2012 *51st IEEE Conference on Decision and Control*, December 10–13, 2012, Maui, HI, United States, p. 3074
[185] Klein R, Chaturvedi N A, Christensen J, Ahmed J, Findeisen R and Kojic A 2013 *IEEE Trans. Control. Syst. Technol.* **21** 289
[186] Han J, Kim D and Sunwoo M 2009 *J. Power Sources* **188** 606
[187] Sun F, Hu X, Zou Y and Li S 2011 *Energy* **36** 3531
[188] Ye M, Guo H and Cao B 2017 *Appl. Energy* **190** 740
[189] Lee K T, Dai M J and Chuang C C 2018 *IEEE Trans. Ind. Electron.* **65** 589
[190] Wu X, Li X and Du J 2018 *IEEE Access* **6** 41993
[191] Liu X, Chen Z, Zhang C and Wu J 2014 *Appl. Energy* **123** 263
[192] Yang F, Xing Y, Wang D and Tsui K L 2016 *Appl. Energy* **164** 387
[193] Li J, Klee Barillas J, Guenther C and Danzer M A 2013 *J. Power Sources* **230** 244
[194] Tian Y, Xia B, Wang M, Sun W and Xu Z 2014 *Energies* **7** 8446
[195] Hu X, Sun F and Zou Y 2013 *Simul. Model. Pract. Theory* **34** 1
[196] Lin C, Tang A and Xing J 2017 *Appl. Energy* **207** 394
[197] Wang J, Liu P, Hicks-Garner J, Sherman E, Soukiazian S, Verbrugge M, Tataria H, Musser J and Finamore P 2011 *J. Power Sources* **196** 3942
[198] Diao W, Saxena S and Pecht M 2019 *J. Power Sources* **435** 226830
[199] He Y J, Shen J N, Shen J F and Ma Z F 2015 *AIChE J.* **61** 1589
[200] Zhou Y, Huang M, Chen Y and Tao Y 2016 *J. Power Sources* **321** 1
[201] Ma C, Zhai X, Wang Z, Tian M, Yu Q, Liu L, Liu H, Wang H and Yang X 2019 *Intl. J. Mach. Learn. Cybern.* **10** 2269
[202] Li J, Lyu C, Wang L, Zhang L and Li C 2014 *J. Power Sources* **268** 895
[203] Weng C, Cui Y, Sun J and Peng H 2013 *J. Power Sources* **235** 36
[204] Galeotti M, Cinà L, Giammanco C, Cordiner S and Di Carlo A 2015 *Energy* **89** 678
[205] Xiong R, Li L and Tian J 2018 *J. Power Sources* **405** 18
[206] Farmann A, Waag W, Marongiu A and Sauer D U 2015 *J. Power Sources* **281** 114
[207] Jiang B, Dai H, Wei X and Xu T 2019 *Appl. Energy* **253** 113619
[208] Hu X, Yuan H, Zou C, Li Z and Zhang L 2018 *IEEE Trans. Veh. Technol.* **67** 10319
[209] Plett G L 2011 *J. Power Sources* **196** 2319
[210] Dong H, Jin X, Lou Y and Wang C 2014 *J. Power Sources* **271** 114
[211] Kim I S 2010 *IEEE Trans. Power Electron.* **25** 1013
[212] Zou Y, Hu X, Ma H and Li S E 2015 *J. Power Sources* **273** 793
[213] Dai H, Xu T, Zhu L, Wei X and Sun Z 2016 *Appl. Energy* **184** 119
[214] Wei Z, Zhao J, Ji D and Tseng K J 2017 *Appl. Energy* **204** 1264
[215] Bartlett A, Marcicki J, Onori S, Rizzoni G, Yang X G and Miller T 2016 *IEEE Trans. Control. Syst. Technol.* **24** 384
[216] Moura S J, Chaturvedi N A and Krstic M 2012 *American Control Conference*, June 27–29, 2012, Montreal, QC, Canada, p. 566
[217] Dey S, Ayalew B and Pisu P 2014 *13th International Workshop on Variable Structure Systems*, June 29–July 2, 2014, Nantes, France, p. 1
[218] Lotfi N, Li J, Landers R G and Park J 2017 *American Control Conference*, May 24–26, 2017, Seattle, United States, p. 86
[219] Zheng L, Zhang L, Zhu J, Wang G and Jiang J 2016 *Appl. Energy* **180** 424
[220] Plett G L 2004 *IEEE Trans. Veh. Technol.* **53** 1586
[221] Farmann A and Sauer D U 2016 *J. Power Sources* **329** 123
[222] Waag W, Fleischer C and Sauer D U 2013 *J. Power Sources* **242** 548
[223] Sun F, Xiong R, He H, Li W and Aussems J E E 2012 *Appl. Energy* **96** 378
[224] Xiong R, Sun F, He H and Nguyen T D 2013 *Energy* **63** 295
[225] Zou C, Klintberg A, Wei Z, Fridholm B, Wik T and Egardt B 2018 *J. Power Sources* **396** 580
[226] Xie J, Ma J and Chen J 2018 *Int. J. Energy Res.* **42** 4730
[227] Zheng L, Zhu J, Wang G, Lu D D C and He T 2018 *IEEE Trans. Power Electron.* **33** 9551
[228] Farmann A and Sauer D U 2018 *Appl. Energy* **225** 1102
[229] Burgos-Mellado C, Orchard M E, Kazerani M, Cárdenas R and Sáez D 2016 *Appl. Energy* **161** 349
[230] Lu J, Chen Z, Yang Y and Lv M 2018 *IEEE Access* **6** 20868
[231] Li Z, Zhang J, Wu B, Huang J, Nie Z, Sun Y, An F and Wu N 2013 *J. Power Sources* **241** 536
[232] Robinson J B, Darr J A, Eastwood D S, Hinds G, Lee P D, Shearing P R, Taiwo O O and Brett D J L 2014 *J. Power Sources* **252** 51
[233] Nascimento M, Ferreira M S and Pinto J L 2017 *Meas. J. Int. Meas. Confed.* **111** 260
[234] Raijmakers L H J, Danilov D L, Eichel R A and Notten P H L 2019 *Appl. Energy* **240** 918
[235] Srinivasan R, Carkhuff B G, Butler M H and Baisden A C 2011 *Electrochim. Acta* **56** 6198
[236] Zhu J G, Sun Z C, Wei X Z and Dai H F 2015 *J. Power Sources* **274** 990
[237] Lin X, Perez H E, Siegel J B, Stefanopoulou A G, Li Y, Anderson R D, Ding Y and Castanier M P 2013 *IEEE Trans. Control. Syst. Technol.* **21** 1745
[238] Zhang C, Li K and Deng J 2016 *J. Power Sources* **302** 146
[239] Sun J, Wei G, Pei L, Lu R, Song K, Wu C and Zhu C 2015 *Energies* **8** 4400
[240] Kim Y, Mohan S, Siegel J B, Stefanopoulou A G and Ding Y 2014 *IEEE Trans. Control. Syst. Technol.* **22** 2277
[241] Dai H, Zhu L, Zhu J, Wei X and Sun Z 2015 *J. Power Sources* **293** 351